JOURNAL OF CATALYSIS **178,** 146–152 (1998)
ARTICLE NO. CA982106

Spectroscopic Evidence of Cu–Al Interactions in Cu–Zn–Al Mixed Oxide Catalysts Used in CO Hydrogenation

R. Tavares Figueiredo, A. Martínez-Arias, M. López Granados, and J. L. G. Fierro[1]

Instituto de Catálisis y Petroleoquímica, CSIC, Campus UAM, Cantoblanco, 28049 Madrid, Spain

Received November 11, 1997; revised February 9, 1998; accepted April 9, 1998

Three different Cu–Zn–Al catalysts (Cu : Zn : Al atomic ratio 60 : 38 : 2) were prepared by coprecipitation of the three metals (from their nitrate salts) either by separately precipitating each metal (Cu + Zn + Al), two metals (Cu and Zn coprecipitated + Al) before mixing together, or by precipitating the three of them together. XPS analysis detected a remarkably high Al enrichment at the surface of all calcined or reduced samples, along with a binding energy of the Cu $2p_{3/2}$ core level peak assigned to Cu^{2+} in $CuAl_2O_4$-like environment in the calcined state. ESR spectra of calcined samples showed signals attributed to surface Cu^{2+} species with Al entities in their surroundings for samples in which Cu and Zn are coprecipitated and aged together. The higher Cu dispersion observed after reduction for these catalysts is attributed to the development of such interactions at the surface of Al-containing calcined samples.

1. INTRODUCTION

$Cu–ZnO–Al_2O_3$ catalysts are used in the industrial methanol synthesis process by the hydrogenation of CO_2 and CO mixtures under relatively low pressure. So far, the best catalytic performance has been achieved with catalysts prepared by coprecipitation of Cu–Zn–Al hydroxycarbonates, followed by calcination under air of the precursor thus obtained and, finally, by activating the catalyst by reduction of the Cu oxide in a H_2 flow prior to feeding the synthesis gas mixture under reaction conditions (1–4). It is now widely accepted that metallic copper particles provide the active sites for the reaction (5–8). The role attributed to ZnO is, basically, to disperse the Cu phase in the calcined sample, in such a way that a high dispersion of Cu metal can be attained when activating the system by reduction; its presence, therefore, leads to a higher amount of active sites exposed to the reaction mixture (1, 3). The favored dispersion of copper in the presence of ZnO is believed to be related to the formation during aging of the coprecipitate, of both aurichalcite, in which Cu^{2+} cations are atomically dispersed in the zinc hydroxycarbonate framework (hydrozincite) and zinchian-malachite, in which Zn^{2+} cations are dispersed in the malachite structure (Cu^{2+} hydroxycarbonate). Then, upon subsequent calcination, decomposition of these precursors leads to the development of small crystallites of CuO, which are the ideal intermediates for obtaining the final reduced catalyst with a high copper dispersion (9). Further contributions to copper dispersion might be related to the disolution of small amounts of isolated Cu^{2+} ions in the ZnO structure (10).

The addition of Al has been reported (1–4) to increase the BET surface area and the Cu dispersion and to decrease the sintering of the Cu particles which occurs under working conditions. However, little or no spectroscopic research has been devoted to clarifying how Al enhances the Cu dispersion. In line with this, it has been proposed that Al^{3+} can also replace Cu^{2+} and Zn^{2+} in the aurichalcite structure during aging of the coprecipitate (11). It can be expected that the interaction between Al^{3+}-containing phases and phases containing Cu^{2+} and Zn^{2+} could be altered by changing the way in which the three metals are coprecipitated and aged together. In this work, different catalysts with a constant Cu : Zn : Al atomic ratio (60 : 38 : 2), but differing in the way the three metals are coprecipitated and aged, are compared. Their characteristics have been analysed by means of N_2O chemisorption, XRD, XPS, and ESR techniques and the catalytic activity in the hydrogenation of CO has been tested.

2. EXPERIMENTAL

2.1. Preparation of Catalysts

The catalysts were prepared, according to a procedure widely reported in the literature (1, 12), via precipitation from aqueous nitrate solutions of Cu, Zn, and Al. The metal nitrate solutions (0.4 *M*) were added dropwise to a vigorously stirred Na_2CO_3 solution (0.3 *M*) at 333 K, maintaining the pH at a value close to 8 by simultaneous addition of Na_2CO_3 solution. Then the precipitates were aged

[1] To whom correspondence should be addressed. E-mail: jlgfierro@icp.csic.es.

0021-9517/98 $25.00

under stirring for more than 30 min at 333 K. The precipitate thus obtained was filtered and extensively washed with deionized water at 333 K until the concentration of Na^+ ions in the filtrate solution was lower than 0.2 ppm, as determined by atomic absorption spectrometry. The precipitate was dried overnight at 383 K (referred to as the precursor), calcined in air at 623 K for 4 h (referred to as the calcined sample), pelletized, and sieved (0.40–0.52 mm) for the characterization experiments and the catalytic runs. All reagents were used as received: $Cu(NO_3)_2 \cdot 3H_2O$ from Johnson Matthey (ACS reagent), $Al(NO_3)_3$ from Fluka (ACS reagent), $Zn(NO_3)_2 \cdot 6H_2O$ from Aldrich (>98%), and Na_2CO_3 from Fluka (MicroSelect reagent).

In this work, three catalysts with the same composition (Cu : Zn : Al, 60 : 38 : 2 atomic ratio) were prepared. The catalyst denominated CZA was prepared by the addition of a solution with the three metal nitrates to the Na_2CO_3 solution. The other two catalysts were obtained as follows: CZ-A by the coprecipitation of copper and zinc nitrates in the basic solution and, after aging of the coprecipitate in the basic solution, addition of the precipitated solution resulting from separate precipitation and aging of Al nitrate. The resultant mixture of precipitates was further aged under agitation. C-Z-A, in turn, was prepared by the precipitation and aging of all the three metals separately, then mixing and aging them under stirring. The washing step was always carried out following aging of the precipitate containing the three metals. A reference catalyst without Al (denoted as CZ) was prepared in a similar method by coprecipitation of copper and zinc nitrates.

2.2. Catalyst Characterization

Powder X-ray diffraction patterns were recorded on a Seifert diffractometer using nickel filtered CuK_α radiation (0.1542 nm). The BET surface area of the catalysts was calculated from the nitrogen adsorption isotherm at 77 K measured in a Micromeritics 2100 automatic apparatus. The chemisorption of nitrous oxide on fresh catalysts was carried out in a Micromeritics TPD/TPR apparatus equipped with a TC detector. Typically, 0.3 g of calcined sample were reduced for 1 h at 493 K in H_2, using a flow rate of 50 ml/min and a ramp of 4 K/min. It is worth noting at this point that preliminary TPR runs carried out in the same equipment had shown that reduction of copper is achieved with this treatment. Then, the sample was cooled down in the reduction mixture at 353 K. Pulses of nitrous oxide diluted in a N_2 flow were admitted flowing through the catalyst at 353 K until no N_2O adsorption was detected. For the calculation, it is assumed that Cu/N_2O stoichiometry is 2 and that the mean atomic surface area for copper is 0.0741 nm^2 (13). The error in the Cu surface area data was estimated to be less than 5%.

ESR spectra at the X band frequency (≈9.5 GHz) were recorded at 77 K with a Bruker ER 200D spectrometer calibrated with DPPH (g = 2.0036). Portions of ca 25 mg of sample are placed inside a quartz probe cell and outgassed at room temperature. Additional experiments were performed after subsequent admission of ambient air (ca 2×10^{-4} mol) on the sample held at 77 K, in order to check the surface nature of the species observed (14). Computer simulations were used to obtain the ESR parameters of some of the signals observed.

XP spectra were acquired with a VG ESCALAB 200R spectrometer equipped with a hemispherical electron analyzer and MgKα (1253.6 eV) X-ray source. The powder samples were reduced *in situ* in the pretreatment by dosing 200 Torr (1 Torr = 133.33 N/m^2) of H_2 at 503 K. Once the XP spectra of the reduced sample are recorded, reoxidation with 200 Torr of O_2 at 623 K was performed in some cases. The intensities were estimated by calculating the integral of each peak after smoothing and subtraction of the "S-shaped" background and fitting the experimental curve to a combination of Lorentzian and Gaussian lines of variable proportions. All binding energies (BE) were referenced to the adventitious C 1s line at 284.9 eV. This reference gave BE values within an accuracy of ±0.2 eV.

2.3. Catalytic Activity Measurements

The catalytic tests were carried out using a tubular stainless steel flow reactor (ID = 10.5 mm). An amount corresponding to 0.6 g of sieved calcined sample was loaded in the reactor and reduced *in situ* with 100 ml/min of 10% H_2/He at 493 K for 1 h; 50 ml/min of H_2 and CO ($H_2/CO = 3$, W/F = 0.2 g · h/mmol of $H_2 + CO$) was used as the reactant mixture, the flow being controlled by means of electronic mass flow controllers. A K-type thermocouple, buried in the catalytic bed, was used to measure and control the temperature. The reactions were conducted at 10 bar overall pressure and reaction temperatures ranging between 453 to 493 K. The effluents of the reactor were analyzed on-line by a Hewlett-Packard 5730 A gas chromatograph equipped with a Poraplot Q and Molecular Sieve X5A columns and TCD and FID. The error in the conversion and selectivity values were estimated to be less than 10%.

3. RESULTS

3.1. Characterization of Precursors, Calcined and Fresh Catalysts

The X-ray diffraction patterns of the precursors showed that all reflections are very weak and broad which indicates poor crystallinity of the phases detected. CZA displays reflections of zinchian-malachite (Cu, $Zn)_2(CO_3)(OH)_2$ (JCPDS 18-1095) and aurichalcite (Cu, $Zn)_5(CO_3)_2(OH)_6$ (JCPDS 17-743). Malachite $Cu_2(CO_3)(OH)_2$ (JCPDS 10-399) and hydrozincite $Zn_5(CO_3)_2(OH)_6$ (JCPDS 10-1458) are probably present as well, but unambiguous assignment

TABLE 1

BET Area of Calcined Samples and Cu Area of Fresh Catalysts

Catalyst	S_{BET} (m^2/g)	S_{Cu} (m^2/g)[a]
CZA	61.0	22.4
CZ-A	65.4	30.0
C-Z-A	55.0	10.8

[a] Metal area as determined by N_2O chemisorption.

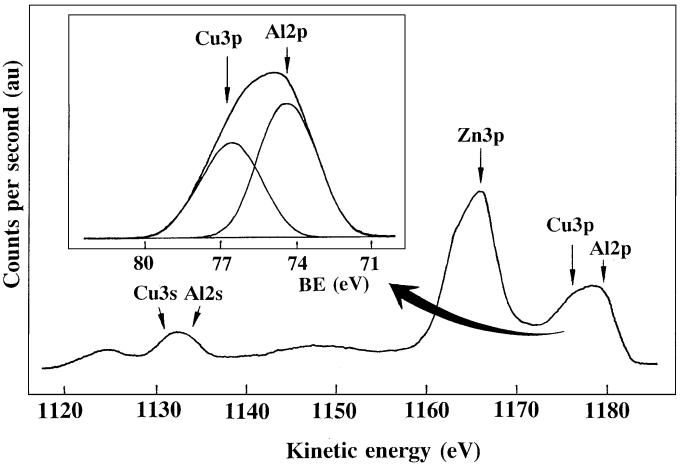

FIG. 1. Wide scan photoelectron spectrum of calcined CZA catalyst. The inset of this figure illustrates the deconvolution procedure applied to measure the Al 2p intensity.

of their reflections cannot be done due to their large widths and to the vicinity of more intense reflection peaks due to zinchian-malachite and aurichalcite, respectively. No Al-containing phase was detected, which might be related to the relatively low amount of this element in the catalysts. It should be recalled that the phases detected correlate well with previous results on systems with similar Cu : Zn : Al composition (9, 12). Like the CZ precursor, also the CZ-A precursor only shows hydrozincite and aurichalcite diffraction peaks. C-Z-A only exhibits malachite reflections and very broad diffraction peak signals of hydrozincite. In this case no detection of zinchian-malachite or aurichalcite is expected, taking into account that such phases are favored when the coprecipited metals are aged together (12). The X-ray diffraction patterns of the calcined samples show that all the samples contained ill-crystallized CuO and ZnO species. Other phases containing any of the metals used in the systems are most likely to be present but, probably due to their poor and highly disordered crystallization or to their small crystal size, they cannot be detected by XRD.

BET areas of calcined catalysts and Cu surface areas of fresh catalysts are compiled in Table 1. The results show that the BET areas for the one-step coprecipitated catalyst CZA and for the two-step coprecipitated catalyst CZ-A are higher than that of C-Z-A. Furthermore, copper surface areas of fresh catalysts were larger for the two catalysts in which both copper and zinc were simultaneously coprecipitated, CZA and CZ-A showing areas roughly two and three times larger, respectively, than C-Z-A.

The chemical state of the components and the relative concentration at the surface have been evaluated by XPS in both calcined and H_2-reduced samples. The surface Cu/M (M = Zn, Al) atomic ratios, summarized in Table 2, have been calculated from peak areas, considering photoelectron cross sections and mean free paths (15, 16). As can be seen in a wide scan of the photoelectron spectrum of the calcined CZA catalyst (Fig. 1), there is overlapping of both Cu 3s–Al 2s and Cu 3p–Al 2p core levels. Due to the overlapping of Cu 3p and Al 2p core level peaks, a deconvolution of both contributions was carried out to quantitatively determine the Al 2p peak intensity. This is illustrated in the inset of Fig. 1. The error in the area value was considered to be ca 10%. The BEs of the most abundant

TABLE 2

XPS Parameters of Copper for Calcined and Fresh Catalysts Subjected to Different Pretreatments

Sample	Pretreatment	BE Cu $2p_{3/2}$	α_A	$(Cu/Zn)_{at}$	$(Cu/Al)_{at}$	FWHM (eV)
CZA	Calcined at 623 K	933.7 (43) 935.1 (57)	1851.7	0.7	1.0	4.6
	Reduced at 503 K	932.5	1851.3	0.3	0.5	
	Reoxidized *in-situ* at 623 K	933.7 (46) 935.3 (54)	1851.6	0.5	0.8	
CZ-A	Calcined at 623 K	933.6 (51) 935.2 (49)	1850.8	1.1	1.2	4.3
	Reduced at 503 K	932.5	1851.2	0.4	0.4	
C-Z-A	Calcined at 623 K	933.4 (73) 935.3 (27)	1850.5	0.7	0.7	3.9
	Reduced at 503 K	932.6	1851.5	0.2	0.4	

Note. Peak percentages are in parenthesis.

elements for different samples are also sumarized in Table 2, along with the full widths at half maximum (FWHM). Cu/Zn ratios are close to those found in the literature for samples with similar Cu/Zn bulk values (9, 10, 17, 18). The largest copper concentration at the surface is observed in the CZ-A sample. Very remarkable data are that the Cu/Al ratios of calcined and reduced samples obtained by XPS are much lower than the bulk Cu/Al ratio which, according to the nominal composition Cu : Zn : Al = 60 : 38 : 2, should be 30. This result indicates that there is an important Al enrichment at the surface. The surface Cu/Al ratio depends on the coprecipitation order but is much smaller than 30 in all samples. The decrease of the Cu/Zn and Cu/Al intensity ratios in H_2-reduced catalysts clearly indicates a lack of copper dispersion as a consequence of Cu particle formation from phases where Cu^{2+} is dispersed on an oxide. Some redispersion of copper takes place on reoxidizing the metallic particles under carefully controlled conditions, as illustrated by the increment of the Cu/Zn intensity ratio in the CZA sample subjected to a complete reduction–oxidation cycle, but the copper dispersion of the original calcined sample is not attained after this cycle in any case.

Figures 2 and 3 show the Cu $2p_{3/2}$ peaks of calcined and hydrogen reduced samples, respectively. From these spectra it is evident that the line profile changes dramatically upon hydrogen reduction at 503 K. The calcined samples (Fig. 2) display the principal Cu $2p_{3/2}$ peak somewhat above

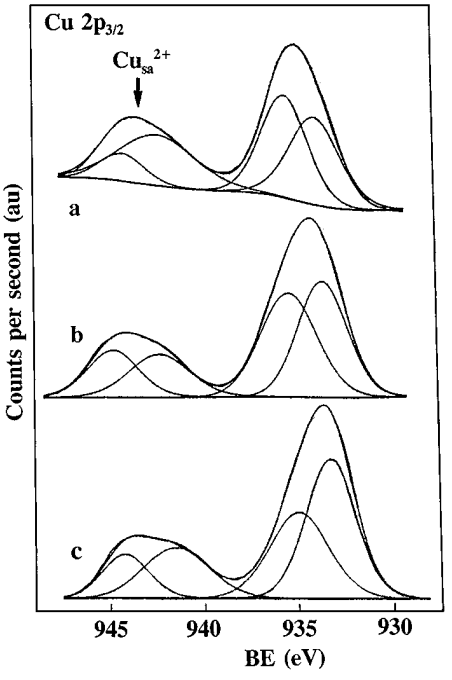

FIG. 2. Cu $2p_{3/2}$ core level spectra of calcined samples: (a) CZA; (b) CZ-A; (c) C-Z-A. Although there is no physical meaning, the shake-up Cu^{2+} satellite placed at 938–948 eV was deconvoluted into two components.

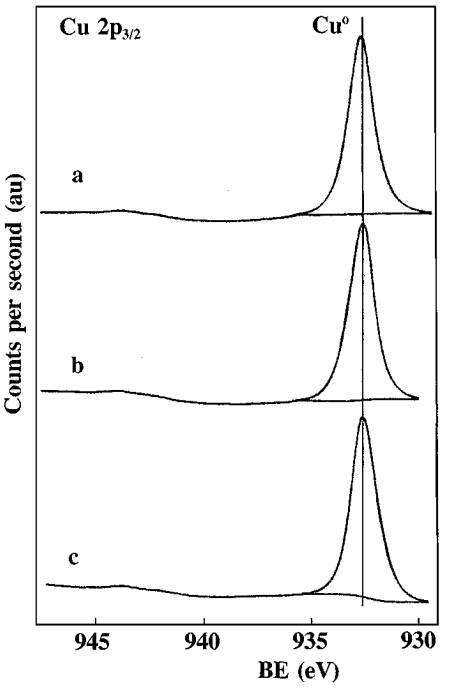

FIG. 3. Cu $2p_{3/2}$ core level spectra of hydrogen-reduced fresh catalysts: (a) CZA; (b) CZ-A; (c) C-Z-A.

934 eV, which is characteristic of Cu^{2+} species (9, 10, 17, 18), when referenced to the C 1s core level at 285.0 eV. An additional means of identifying Cu^{2+} ions is the satellite line of the principal, whose origin is complex and has been explained as due to electron shake-up processes (19, 20), final state effects (21, 22), and charge transfer mechanisms (23). The value of the FWHM of Cu $2p_{3/2}$ peak for calcined samples is larger than those of other similar Al-free calcined samples prepared in our laboratory and analyzed in our electron spectrometer (24). This suggests that the Cu $2p_{3/2}$ peak of Al-containing samples in this work may consist of more than one contribution (BE and FWHM of both Al 2p and Zn $2p_{3/2}$ peaks were constant irrespective of sample, implying that the change in the FWHM of the Cu $2p_{3/2}$ level was not due to differential charging). On this basis, peaks of calcined samples have been deconvoluted into two contributions centered around 933.5 and 935.1 eV. The latter peak, which is most abundant in CZA and CZ-A, is assigned to Cu^{2+} in a $CuAl_2O_4$ spinel-like environment (25), whereas the peak at 933.5 eV is attributed to Cu^{2+} in CuO.

The disappearance of the satellite peak and the simultaneous shift of the principal Cu $2p_{3/2}$ peak towards lower BE upon H_2 reduction at 503 K show that after reduction the copper species are Cu^+ or Cu^0, but not Cu^{2+}. Since the BE values and widths for Cu 2p peaks in cuprous oxide (Cu^+) and Cu^0 are almost identical, the distinction between Cu^+ and Cu^0 species present in the catalyst is only feasible through examination of the modified Auger parameter.

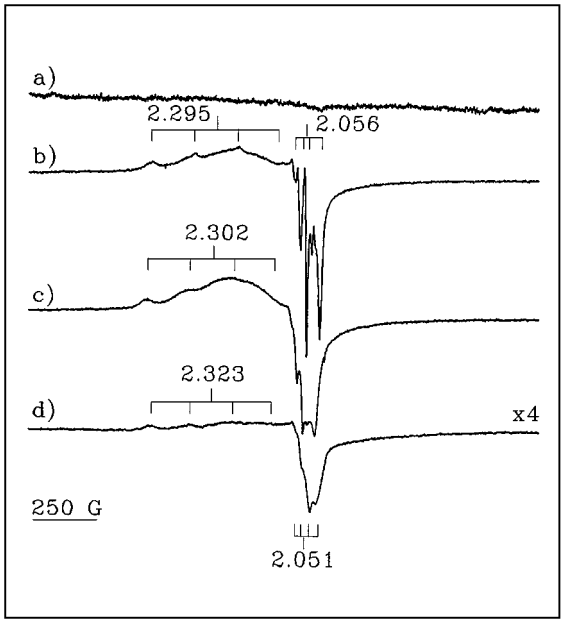

FIG. 4. ESR spectra of air-calcined samples: (a) C-Z-A; (b) CZ-A; (c) CZA; (d) CZ.

The modified Auger parameter is defined by the equation: $\alpha_{A'} = h \cdot \upsilon + (Cu_{LMM} - Cu\,2p)$, where the parameter $\alpha_{A'}$ represents the difference between the kinetic energy of the Cu_{LMM} Auger electron and the Cu $2p_{3/2}$ photoelectron. Table 2 shows $\alpha_{A'}$ values at 1851.2–1851.6 eV, which are characteristic of Cu^0 species (26).

ESR spectra of calcined samples are shown in Fig. 4. No signal can be discerned after this treatment for the C-Z-A sample, Fig. 4a. In contrast, ESR signals are observed both for CZ-A and CZA, Figs. 4b and 4c. The spectra of these samples consist of two overlapping signals: signal A, showing a resolved hyperfine pattern of four peaks in the parallel as well as perpendicular components, and signal B, showing broad structureless features. Thus, the spectrum of CZ-A shows a major contribution from a narrow axial signal A with $g_\parallel = 2.295$, $g_\perp = 2.056$, $A_\parallel = 18.4 \times 10^{-3}$ cm^{-1} (172 G) and $A_\perp = 2.1 \times 10^{-3}$ cm^{-1} (22 G), while for CZA the main contribution to the spectrum is due to a broad signal B, showing extremes at $g = 2.23$ and $g = 2.05$; signal A, showing slightly modified parameters ($g_\parallel = 2.302$, $g_\perp = 2.055$, $A_\parallel = 18.5 \times 10^{-3}$ cm^{-1} (172 G) and $A_\perp = 1.9 \times 10^{-3}$ cm^{-1} (20 G)) and somewhat broader features than in CZ-A, overlaps with signal B (Fig. 4c). Admission of air to these samples leads to a significant broadening of the features due to type A signals and an apparent decrease in the intensity of signal B, indicating the surface character of the corresponding species.

Both signals A and B are typical of Cu^{2+} ions. Signal B, showing unresolved hyperfine splittings, can be attributed in a generic way to clustered Cu^{2+} species, its large linewidth being due to magnetic interactions between the Cu^{2+} ions. Although, due to the lack of spectral details, assignment to a specific Cu^{2+}-containing phase is difficult, its similarity to a signal observed on Cu/Al_2O_3 samples suggests that it can be assigned to clustered Cu^{2+} in a $CuAl_2O_4$ spinel-like phase (27). The attribution to a well crystalized CuO phase can be discarded since strong magnetic interactions between Cu^{2+} ions in this phase yields ESR-silent species (28). Signal A, on the other hand, must be attributed to isolated Cu^{2+} ions, in view of its well-resolved hyperfine splitting, which results from hyperfine coupling between the 3d unpaired electron and the copper ($I = 3/2$) nuclear spin, its presence indicating the absence of strong magnetic interactions with its environment. Its ESR parameters are typical of isolated Cu^{2+} ions in sites of octahedral symmetry with tetragonal distortions (axial lengthening and planar shortening). Signals of this kind have been obtained in Cu–Zn (29, 30) and Cu–Zn–Al (31) mixed oxides. However, in these cases higher $g_\parallel$ and lower $A_\parallel$ values were obtained for signals, which indicates that the environment of the corresponding Cu^{2+} ions was different than for those giving signal A. Earlier assignment to isolated Cu^{2+} in the lattice of the spinel phase $ZnAl_2O_4$ (31) seems unlikely, in view of the similarities of the parameters observed in that work and those observed for similarly pretreated Cu–Zn mixed oxides (29, 30). Taking these results into account, the differences between signal A and signals due to isolated Cu^{2+} species in Cu–Zn mixed oxide systems can be considered as being due to the presence of aluminum cations in the environment of signal A. Further support to this assignment comes from an additional experiment performed on a calcined Al-free sample (CZ). Figure 3d shows the spectrum which presents an axial signal A′ due to isolated Cu^{2+} species similar to those observed previously (29–31) with $g_\parallel = 2.323$, $g_\perp = 2.051$, $A_\parallel = 16.8 \times 10^{-3}$ cm^{-1} (155 G), and $A_\perp = 2.4 \times 10^{-3}$ cm^{-1} (25 G); it is worth noting that the overall intensity is lower than that of the spectra of CZA or CZ-A (Figs. 4b and 4c). Signal A′ also suffers a significant broadening on admission of air which reveals its surface or close to surface character. From these results, a plausible assignment for signal A would be isolated Cu^{2+} ions influenced by the presence of close Al^{3+} ions; since surface isolated Cu^{2+} interacting with pure γ-Al_2O_3 shows somewhat higher $g_\parallel$ and lower $A_\parallel$ values (27), the possibility that some of the ligands involves zinc cations or incompletely decomposed ligands cannot be fully discarded.

3.2. Catalytic Properties

Table 3 summarizes the catalytic behavior of all catalysts at 493 K. It can be seen that, even though CO_2, methane, ethanol, C_2, and C_3 hydrocarbons were also detected, the catalysts are quite selective to methanol but at a very low yield. The most methanol selective catalysts are CZA and CZ-A. It is worth noting that higher conversion could have been achieved by using CO–CO_2 mixtures as in

TABLE 3

Catalytic Properties at 493 K and 10 bars in CO Hydrogenation and Cu Area of Catalysts

Catalyst	Conversion (mmol/h × kg_{ca})	%S CH_3OH	%S CO_2	%S CH_4	%S C_2	%S C_3–C_4	%S CH_3CH_2OH	S_{Cu} (m^2/g)
CZA	1723	96.8	1.9	0.7	0.4	0.2	0.0	7.9
CZ-A	1490	99.2	0.0	0.4	0.2	0.1	0.1	11.7
C-Z-A	664	89.9	4.8	3.2	1.0	1.1	0.0	7.1

the industrial process. However, our approach consisted in establishing differences in performance among the catalysts prepared by different routes. Used catalysts were then withdrawn from the reactor, and the area of exposed Cu measured by N_2O chemisorption, after re-reduction in H_2, according to the usual method, at 493 K. The results, presented in Table 3, show that the Cu area of used catalysts is smaller than that of fresh catalysts. Considering that equilibrium conditions were attained by the reduction procedure used to prepare the fresh catalyst, it can be assumed that no further increase of particle sizes in respect to those observed for the fresh catalysts is going to be produced on the used catalysts by performing a second treatment in H_2. Further interferences in this measurement by the presence of formates or carbonate-type species adsorbed on the copper particles is not expected, since such species are eliminated by this reduction treatment (32). Thus, this result gives a measure of the changes produced in the Cu particles under reaction conditions, indicating that Cu sinterization is produced by interaction with the reactant mixture. The Cu area depletion is larger in CZA and CZ-A fresh catalysts, the samples with higher initial Cu areas, although CZ-A still shows the higher Cu area.

4. DISCUSSION

Among all the data presented in this work, two characterization results must be emphasized. First, the remarkably high Al concentration found in all systems by XPS analysis, which strongly suggests that Al^{3+} is concentrated in the regions close to the surface of the samples. The fact that the XPS Cu/Al atomic ratio is quite similar in all preparations is somewhat surprising; even in the C-Z-A sample, in which the value of the Cu/Al ratio of the physical mixture would have been expected. The Cu/Al atomic ratios of the systems in this work are close to values reported in the literature (18) for samples much richer in Al. The results obtained suggest in any case that a surface enrichment in Al^{3+} cations is produced probably during calcination of the samples. The presence of an XPS signal at 935.3–935.1 eV, assigned to Cu^{2+} in the $Cu_2Al_2O_4$-like environment, further supports the hypothesis of the occurrence of surface Al-enrichment, since otherwise such a spinel-like environment would hardly have been detected.

The second remarkable result is the detection by ESR of surface Cu^{2+} centers isolated and interacting with aluminum entities for CZA and CZ-A calcined samples. In the case of calcined C-Z-A, Cu^{2+} ions are most likely forming well-crystallized CuO phases that would give rise to ESR-silent species, due to strong magnetic interactions between the Cu^{2+} ions (28). The CZ calcined sample does not seem to present signal B, which suggests that this signal might also be related to the presence of Al in the system. In this sense, it seems reasonable that signal B, detected for CZA and, to a lesser extent, in CZ-A, arises from Cu^{2+} in the $CuAl_2O_4$ phase (27). On the other hand, the possibility that some of the ligands of isolated Cu^{2+} ions giving signal A involve Zn^{2+} cations (probably with oxygen anions bridging both cations) cannot be fully rejected.

It is worth noting that fresh catalysts with higher Cu dispersions (CZA and CZ-A) are those which present evidence of Cu–Al interactions at their surfaces in the calcined states of the samples. In view of these coincident results, it can be proposed that the presence of aluminum contributes to a significant extent to the dispersion of entities of oxidized copper at the surface of the calcined samples, both by the formation of specific surface phases between copper and aluminum and by the stabilization of isolated Cu^{2+} species. Then, upon subsequent reduction, these dispersed cations might behave as anchoring points for the formation of copper particles (33), leading to higher Cu surface areas and, consequently, to higher catalytic activities.

ACKNOWLEDGMENTS

This work was supported by the CICYT, Spain, under Grant MAT95-0894. One of us (R.T.F.) acknowledges a Grant from CNPq, Brazil. The assistance of Mr. E. Pardo in recording photoelectron spectra is acknowledged. We thank Professor J. Soria for the use of the ESR spectrometer.

REFERENCES

1. Bart, J. C., and Sneeden, R. P., *Catal. Today* **2**, 1 (1987).
2. Chinchen, G. C., Denny, P. J., Jennings, J. R., Spencer, M. S., and Waugh, K. C., *Appl. Catal.* **36**, 1 (1989).
3. Chinchen, G. C., Mansfield, K., and Spencer, M. S., *Chemtech*, Nov., 693 (1990).
4. Herman, R. G., *in* "New Trends in CO Activation," Stud. Surf. Sci. Catal. (L. Guczi, Ed.), Chap. 7. Elsevier, Amsterdam, 1991.
5. Waugh, K. C., *Catal. Today* **15**, 51 (1992).

6. Chinchen, G. C., Spencer, M. S., Waugh, K. C., and Whan, D. A., *J. Chem. Soc. Faraday Trans. I* **83**, 2193 (1987).
7. Rasmussen, P. B., Kazuta, M., and Chorkendorff, Y., *Surf. Sci.* **318**, 313 (1995).
8. Yosihara, J., Parker, S. C., Schafer, A., and Campbell, C. T., *Catal. Lett.* **31**, 313 (1995).
9. Porta, P., Campa, M. C., Fierro, G., Lo Jacono, M., Minelli, G., Moretti, G., and Stoppa, L., *J. Mater. Chem.* **3**, 505 (1993).
10. Herman, R. G., Klier, K., Simmons, G. W., Finn, P. B., Bulko, J. B., and Kobylinski, T. P., *J. Catal.* **56**, 407 (1979).
11. Sengupta, G., Sharma, R. K., Sharma, V. B., Mishra, K. K., Kundu, M. L., Sanyal, R. M., and Dutta, S., *J. Solid State Chem.* **115**, 204 (1995).
12. Fujita, S., Satriyo, A. M., Shen, G. C., and Takezawa, N., *Catal. Lett.* **34**, 85 (1995).
13. Evans, J. W., Wainwright, M. S., Bridgewater, A. J., and Young, D. J., *Appl. Catal.* **7**, 75 (1983).
14. Che, M., and Tench, A. J., *Adv. Catal.* **32**, 1 (1983).
15. Scoffield, J. H., *J. Electron Spectros. Related Phenom.* **8**, 129 (1976).
16. Penn, D. R., *J. Electron Spectros. Related. Phenom.* **9**, 29 (1976).
17. Okamoto, Y., Fukino, K., Imanaka, T., and Teranishi, S., *J. Phys. Chem.* **87**, 3740 (1983).
18. Garbassi, F., and Petrini, G., *J. Catal.* **90**, 113 (1984).
19. Fiermans, L., Hoogewijs, R., and Vennik, J., *Surf. Sci.* **47**, 1 (1975).
20. Kim, K. S., *J. Electron Spectrosc. Relat. Phenom.* **3**, 217 (1974).
21. Van der Laan, G., Westra, C., Haas, C., and Sawatzky, G. A., *Phys. Rev. B* **23**, 4369 (1981).
22. Okada, K., and Kotani, A., *J. Electron Spectr. Relat. Phenom.* **86**, 119 (1997).
23. Parmigiani, F., and Sangaletti, L., *J. Electron Spectr. Relat. Phenom.* **66**, 223 (1994).
24. Alejo Espinoza, L., Ph.D. thesis, Autonomous University of Madrid, Madrid, 1996.
25. Sepúlveda, A., Márquez, C., Rodriguez-Ramos, I., Guerrero-Ruíz, A., and Fierro, J. L. G., *Surf. Interface Anal.* **20**, 1067 (1993).
26. Fierro, J. L. G., *Catal. Rev.-Sci. Eng.* **34**, 255 (1993).
27. Martínez-Arias, A., Cataluña, R., Conesa, J. C., and Soria, J., *J. Phys. Chem. B* **102**, 809 (1998).
28. Mehran, F., Barnes, S. E., Chandrashekhar, G. V., Mc Guire, T. R., and Shafer, M. W., *Sol. State Commun.* **67**, 1187 (1988).
29. Giamello, E., Fubini, B., and Lauro, P., *Appl. Catal.* **21**, 133 (1986).
30. Andreev, A. A., Kalchev, M. G., Christov, G. D., and Andreeva, D. Ch., *Kinet. Katal.* **36**, 828 (1995).
31. Kaltchev, K., Christov, G., and Andreev, A. A., *in* "Proc. 6th International Symposium on Heterogeneous Catalysis, Sofia, 1987," Part 2, p. 405.
32. Chorkendorff, Y., Rasmussen, P. B., Christoffersen, H., and Taylor, P. A., *Surf. Sci.* **287**, 208 (1993).
33. Louis, C., Cheng, Z. X., and Che, M., *J. Phys. Chem.* **97**, 5703 (1993).